CEAMPP 2013

3rd National Conference on Electronic, Atomic, Molecular and Photonic Physics
Belgrade, Serbia, August 25th, 2013

# CONTRIBUTED PAPERS

&

# ABSTRACTS OF INVITED LECTURES AND PROGRESS REPORTS

University of Belgrade

Faculty of Physics

Editors
B.P. Marinković, G.B. Poparić

University of Belgrade, Faculty of Physics,
Belgrade, Serbia

# CEAMPP2013

# CONTRIBUTED PAPERS

# &

# ABSTRACTS OF INVITED LECTURES
# AND
# PROGRESS REPORTS

August 25th, 2013. Belgrade, Serbia

Editors
Bratislav P. Marinković, Goran B. Poparić

Publisher:
University of Belgrade, Faculty of Physics,
Studentski trg 12, 11000 Belgrade, Serbia



**Printed by: SKRIPTA INTERNACIONAL**

CIP - Каталогизација у публикацији
Народна библиотека Србије, Београд

539.1(048)

NATIONAL Conference on Electronic, Atomic, Molecular and Photonic Physics (3rd ; 2013 ; Beograd)
Contributed Papers & Abstracts of Invited Lectures and Progress Reports / 3rd National Conference on Electronic, Atomic, Molecular and Photonic Physics, CEAMPP 2013, Belgrade, August 25th, 2013 ; [organized by] University of Belgrade, Faculty of Physics [with support of Ministry of Education, Science and Technological Development Republic of Serbia] ; editors B.[Bratislav] P. Marinković, G.[Goran] B. Poparić. - Belgrade : Faculty of Physics, 2013 (Belgrade : Skripta internacional). - XX, 52 str. : ilustr. ; 25 cm

Tiraž 100. - Str. III: Preface / editors. - Bibliografija uz svaki rad. - Registar.

ISBN 978-86-84539-10-8
1. Marinković, Bratislav P., 1956- [уредник] [аутор додатног текста] 2. Faculty of Physics (Beograd)
a) Атомска физика - Апстракти b) Молекуларна физика - Апстракти
COBISS.SR-ID 200134924

# CONTRIBUTED PAPERS

# Red shift in 6 pictures

D. Šević[1], M.S. Rabasović[1], M. Terzić[2], and B.P. Marinković[1]

[1]*Institute of Physics, University of Belgrade, Belgrade, Serbia*

[2] *Faculty of Science, University of Novi Sad, Serbia*

e-mail: sevic@ipb.ac.rs

**Abstract** Self absorption phenomenon plays a very important role in the emission properties of the fluorescent dyes. In the geometry of our laser induced fluorescence experiment, the distance of the excitation beam from the surface of the cuvette that is facing the detection system is very important. To analyze the effects of self absorption phenomenon in our experimental set-up we used Rhodamine B and Eosin ethanol solutions. OPO tuned excitation at 475 nm was used to excite samples.

## INTRODUCTION

Self absorption phenomenon plays a very important role in the emission properties of the fluorescent dyes ([1] and references therein). In the geometry of our experiment, the distance of the excitation beam from the surface of the cuvette is very important. As the excitation goes deeper from the surface that is facing the detection system the emission from the molecules encounters larger number of ground state molecules and hence more absorption of the shorter wavelength side emission. To analyze the effects of this phenomenon in our experimental set-up we used Rhodamine B and Eosin ethanol solutions. OPO tuned excitation at 475 nm was used to excite samples.

The basic setup of our time resolved laser induced fluorescence experiment consists of Nd-YAG Vibrant OPO laser system and Hamamatsu streak camera. The output of the OPO can be continuously tuned over a spectral range from 320 nm to 475 nm. It is possible to excite the samples also by using the Nd-YAG output (1064 nm) and the second and fourth harmonics. The system is suitable and used additionally for laser induced breakdown spectroscopy (LIBS). The emission spectra are recorded using a streak scope (Hamamatsu model C4334-01) with integrated video streak camera. A detailed description of our TR-LIF/LIBS and recent results are published elsewhere [2-6].

The fluorescence emission is collected at $90^{o}$ from the excitation and dispersed by a 0.3 m focal length triple grating imaging spectrograph (SpectraPro-2300i). For measurements presented here the grating of 50 g/mm was used covering a 330 nm spectral range. The fluorescence spectra are recorded at room temperature.

## RESULT AND DISCUSSION

The streak images of fluorescent spectra of Rhodamine B ethanol solution are presented in Fig 1. Measurements were made in photon counting mode of streak camera, so intensities of signal correspond to number of detected photons. Although all experimental parameters except for the distance of the excitation beam from the detecting surface of the cell were exactly the same (excitation energy of 5 mJ and excitation wavelength of 475 nm, the same sample, Rhodamin B ethanol solution of concentration of $5x10^{-3}$ M), the streak images look very different. Distances of the excitation beam from the detecting surface of the cell were approximately 1mm, 2mm, … 6 mm, as denoted by A, B, … F in Fig 1. It should be noted that the shift of spectra could be estimated not only

by peak position, but also by the shape of left and right side of spectra. OPO excitation at 475 nm is also visible on Figs 1 and 2.

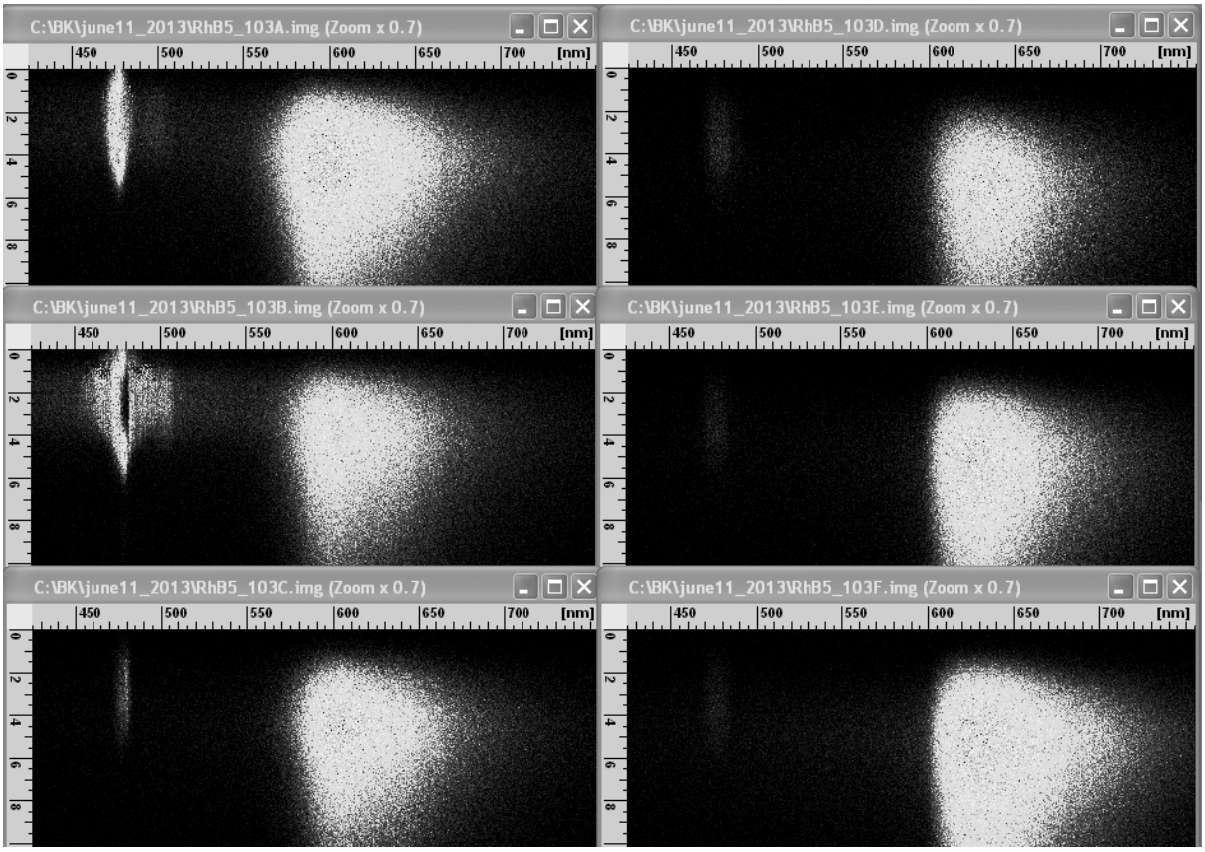


Fig 1. The streak images of fluorescent spectra of Rhodamine B ethanol solution, concentration of $5x10^{-3}$ M. Excitation energy is 5 mJ and excitation wavelength is 475 nm. Distances of the excitation beam from the detecting surface of the cell are approximately 1mm, 2 mm, … 6 mm, as denoted by A, B,C (top to bottom left side), D,E,F (top to bottom right side). OPO excitation is visible at 475 nm, barely discernable at thicker optical paths, D,E and F.

Intensities of measured spectra are usually presented in pseudocolor. In greyscale images shown in Figs 1 and 2, the visual intensity of the image corresponds to signal intensity.

The streak images of fluorescent spectra of Eosin ethanol solution of concentration of about $5x10^{-4}$ M are presented in Fig 2. Again, all experimental parameters except for the distance of the excitation beam from the detecting surface of the cell were exactly the same, the same as for Rhodamine B. Distances of the excitation beam from the detecting surface of the cell were approximately 1mm, 2mm and 3 mm, as denoted by A, B and C in Fig 2. The red shift is less visible than on the Fig 1, pronounced mainly on the right side of spectra. Images for larger distances than 3 mm show insignificant red shift and are not presented here.

Comparing measurements presented in Fig 1 and Fig 2 it is easy to confirm that the red shift depends (among many other conditions) on the kind of fluorescent dye used and its concentration. Purpose of the measurements presented in Fig 2 is to confirm that it is possible to measure fluorescence in standard 10 mm optical path cuvette without significant red shift.

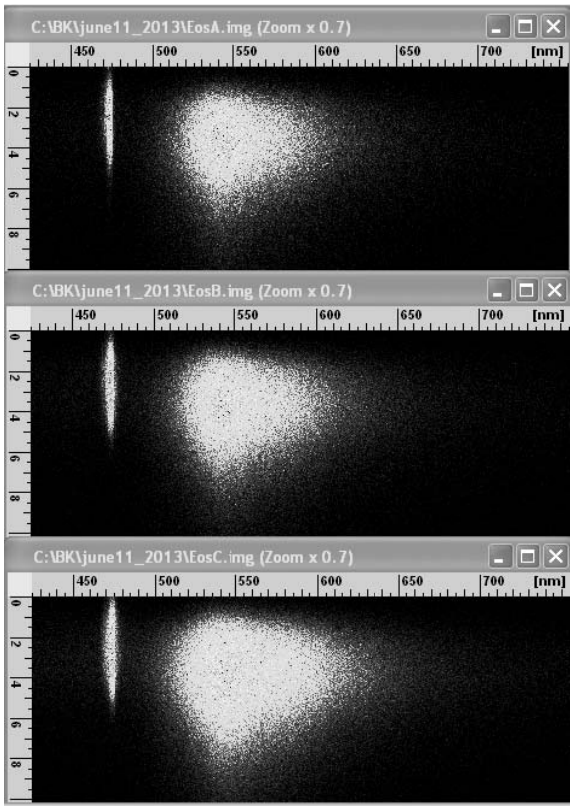


Fig 2. The streak images of fluorescent spectra of Eosin ethanol solution of concentration of about $5x10^{-4}$ M. Excitation energy is 5 mJ and excitation wavelength is 475 nm. Distances of the excitation beam from the detecting surface of the cell are approximately 1mm, 2 mm and 3 mm, as denoted by A, B and C (top to bottom). OPO excitation is visible at 475 nm.

CONCLUSIONS

In our measurements, the red shift was more pronounced for Rhodamine B than Eosin ethanol solution. In many but not all situations, the usual way to alleviate the problem caused by red shift is achieved by using the standard cuvette holder. In this way, different measurements could be compared under the same conditions. Another approach is to minimize the red shift. It could be accomplished by putting the dye solution between the two pressed glass plates, or, even better, using 1 mm x 10 mm cuvette obtaining very thin sample to be measured.

*Acknowledgments:* This work has been done within the project RS OI 171020 partially financed by MESTD

REFERENCES

[1] Fikry M, Omar MM, Ismail LZ (2009) J. Fluoresc. **19** 741-746
[2] M. S. Rabasovic, D. Sevic, V. Pejcev, B. P. Marinkovic, Nucl.Instrum. Meth. B. **279** 58-61 (2012).
[3] M. S. Rabasovic, D. Sevic, M. Terzic, B. P. Marinkovic, Nucl.Instrum. Meth. B. **279** 16-19 (2012).
[4] M. S. Rabasović, D. Šević, M. Terzić, B. P. Marinković, Phys. Scr. **T149** 014076 (2012).
[5] D. Sevic, M. S. Rabasovic, B. P. Marinkovic, IEEE Trans. Plasma Sci. **39(11)** 2782-2783 (2011).
[6] M. S. Rabasovic, D. Sevic, M. Terzic, S. Savic- Sevic, B. Muric, D. Pantelic and B.P. Marinkovic, Acta Physica Polonica A **116** (4) 570 – 572 (2009).

# Electron impact studies of autoionizing states and resonances in helium

J. J. Jureta, A. R. Milosavljević and B. P. Marinković
*Laboratory of atomic colission processes, Institute of Physics,University in Belgrade, Pregrevica 118a, 11080 Belgrade, Serbia*

**Abstract.** Autoionizing states and resonances in helium lying above the first ionization limit (24.587 eV) have been extensively studied in the past by electron impact [1,2]. Helium is the second atom on which we have continued our studies on autoionization processes by using electron spectrometer OHRHA described earlier [3].

## EXPERIMENT

The spectrometer OHRHA consists of a high energy electron gun, a high resolution hemispherical analyzer, a hypodermic needle as a source of an effusive beam of target gas and a Faraday cup as a collector for the electron beam. The electron gun is designed by Omicron VakuumphysikGmbh for electron impact energies from 10 eV to 2.5 keV with a resolution of 0.5 eV and the electron current of several micro Amperes (1 to 15μA). In the present measurements its position is fixed at the angle of 90° with respect to the gas beam. The hemispherical energy analyzer (EA 125 HR, Omicron) has a mean radius of 125 mm and variable entrance/exit slits. It is equipped with 7 channeltrons for detection of ejected electrons. Ultimate projected energy resolution is of the order of 10 meV depending on the type of experiment (XPS, AUGER and EIS).

## RESULT AND DISCUSSION

The representative ejected electron spectra measured at the electron scattering angle of $90^{o}$ are shown in Figure 1. The incident electron energies i.e. excitation energies are shown on the left hand side on the figure from 58.3 to 996 eV. The calibration point for ejected energy scale was taken from the position of the double excited $2s2p(^{1}P)$ state at 60.130 eV [4] (35.54 eV ejected energy).The four lowest n=2 levels are shown in the left part of the figure while the other states below n=2 limit at 65.377 eV [5] (40.79 eV ejected energy) are shown on the right part of the figure. The form of autoionizing states changes drastically with electron excitation energies due to the presence of nearby resonances. The influence of resonances on the states and their angular analysis in the range from 10 to 120 degrees will be present at the conference.

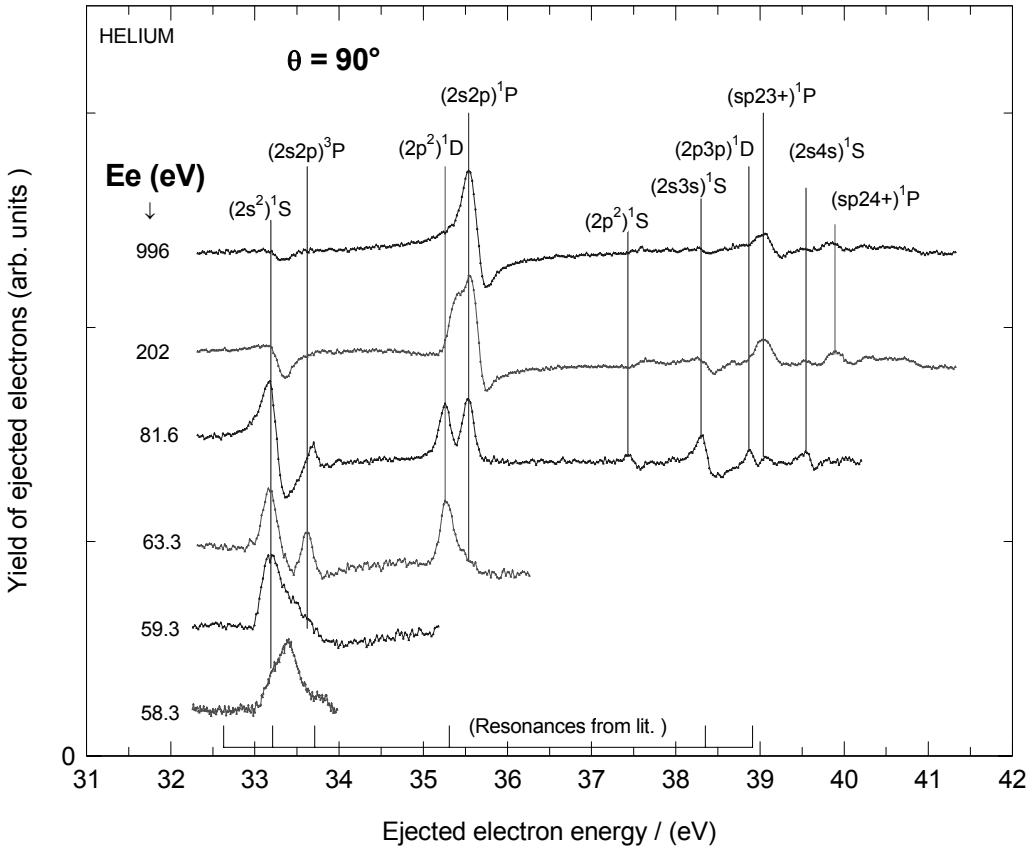


**Figure 1.***Ejected electron spectra of helium obtained at the ejection angle of 90°. The incident electron energies, Ee, are shown on the left hand side on the figure ranging from 996 to 58.3 eV respectively. Energy width per channel was 0.020 eV. Resonances from literature [2] are shown on the bottom of the figure.*

ACKNOWLEDGMEENTS

This work has been done within the projects MESTD RS #OI 171020 and COST Action CM1204 "XUV/X-ray light and fast ions for ultrafast chemistry (XLIC)".

REFERENCES

[1] P.J.Hicks, S. Cvejanović, J. Comer, F. H. Read and J. M. Sharp, *Vacuum***24**, 573 (1974).
[2] S. J. Buckman and C. W. Clark, *Rev. Mod. Phys*. **66**, 539-665 (1994).
[3] J. J. Jureta, A. R. Milosavljević and B. P. Marinković, *Proc*. 2nd*Conference on Electronic, Atomic, Molecular and Photonic Physics* (CEAMPP 2011), Belgrade, Serbia, June 21 – 25, 2011, CEPAS 2011 & CEAMPP 2011 Contributed Papers & Abstracts of Invited Lectures, Eds. A. R. Milosavljević, S. Dujko and B. P. Marinković, p. 126. ISBN: 978-86-82441-32-8
[4] R. P. Madden and K. Codling, *Phys. Rev. Lett.***10**, 516-518 (1963).
[5] A. Crowe, D. G. McDonald, S. E. Martin and V. V. Balashov, *Can. J. Phys.***74**, 736-742 (1996).

# Characterization of low-energy electrons produced upon electron passing through a single Teflon capillary

A. R. Milosavljević[1,*], R. J. Bereczky[2], J. B. Maljković[1], K. Tőkési[2], B. P. Marinković[1]
[1]*Institute of Physics Belgrade, University of Belgrade, Pregrevica 118, 11080 Belgrade, Serbia*
[2]*Institute for Nuclear Research, Hungarian Academy of Sciences, H-4001 Debrecen, Hungary, EU*
* e-mail: vraz@ipb.ac.rs

**Abstract** The transmission of 200 eV and 250 eV electrons through a single Teflon capillary, particularly the yield of low-energy electrons (close to 0 eV) escaping the capillary was investigated. We measured the kinetic energy distribution of the outgoing electrons, as well as the dependence of the low-energy electron current as a function of the angle between the incident electron beam and the capillary axis (tilt angle). We found that a large amount of low-energy electrons is produced within the capillary and their intensity is practically independent on the tilt angle.

## INTRODUCTION

The transmission of charged particles through insulating nano- and micro-capillaries has been intensively investigated in recent years. The first experiment was reported in 2002 by Stolterfoht and coworkers [1], who found a remarkable guiding effect of 3 keV $Ne^{7+}$ highly charged ions (HCI) by highly insulating polyethylene terephthalate (PET) nanocapillaries. The large number of papers followed afterwards devoted to investigation of both fundamental properties of the discovered HCI guiding effect and possible applications. A comprehensive review, including both HCI and electron guiding, can be found in a recent work by Lemell et al. [2]. The physical picture of the HCI guiding is intuitively clear and well understood. The incident beam of highly charged particles enters the insulating capillary and produces charged patches on the wall inside the capillary, so after an initial charge-up time, the beam can be effectively steered (guided) along the capillary axis, even if it is tilted with respect to the incident direction. The guiding effect is actually the result of a process of a self-organized charge-up of the capillary wall, which subsequently deflects ions electrostatically and prevents close collisions with the walls. This process has been well proved experimentally and explained/simulated theoretically [2]. Very interesting applications emerged from this effect, for example, a possibility to introduce a micro/nano HCI beam directly into a biological object (e.g. a cell) [3].

However, in contrary to guiding of HCI by insulating capillaries due to formation of charged patches and Coulomb deflection, the transmission of electrons through insulating capillaries appeared to be more complex. A general opinion is that both the Coulomb deflection (as in the HCI case) and an electron-wall interaction contribute to the process. The first results on electron guiding through insulating nanocapillaries have been published more recently [4,5], and a large interest has been devoted to this topic since then (see [2], for a review). Particularly, the investigation of transmission of electrons through insulating nanocapillaries might shed further light on the topic and brings new applications. Most of the work on electron guiding has been performed to investigate elastically transmitted electrons through nanocapillary arrays or single microcapillaries, as an analogue to the HCI guiding. The inelastic processes have been also reported. Particularly, high-resolution measurements by Milosavljevic et al [6,7] have shown that a large fraction of electrons escaping the

capillary possess very low kinetic energies (close to 0 eV). Nevertheless, according to our knowledge, the properties of these low-energy electrons produced by the insulating nanocapillaries have not been investigated so far in details. In the present work, we report preliminary results on the characterization of electrons at kinetic energies close to 0 eV escaping the long Teflon microcapillary. We believe that our work might bring new insights into the electron guiding, and lead to interesting applications – for example, a possibility to introduce very low-energy (fairly monochromatized) micro/nano electron beam into a dense environment or close to the surface.

## EXPERIMENTAL SETUP

The straight Teflon capillary has been prepared at the Institute for Nuclear Research, Hungarian Academy of Sciences (Atomki) laboratory in Debrecen, Hungary. The sample was fixed into an aluminium holder (see Figure 1) and UHV compatible glue was used to fix the tubes. The capillary has the inner diameter of d=0.8 mm, the outer diameter of 1.6 mm and the length of l=44.15 mm, therefore, the aspect ratio (l/d) is 55.2. The front and back surfaces of the capillary have been coated with graphite in order to prevent charge build up.

The experiment has been performed in the Laboratory for Atomic Collision Processes, at the Institute of Physics Belgrade (IPB). The electron spectrometer UGRA, usually used for electron/atom (molecular) collision experiments, has been modified as described before [4,6,7] in order to investigate electron transmission through capillary samples. Briefly, the electron gun produces a well collimated electron beam, with a diameter and an angular divergence estimated to be approximately 1 mm and $1^o$ at 200 eV of the incident energy, and with an energy spread of about 0.5 eV. The electrons escaping the capillary were focused into a double cylindrical mirror energy analyzer, followed by a single channel multiplier used as a detector. The capillary holder (see Figure 1) has been positioned to have the capillary exit close to the first grounded electrode of the entrance lens preceding the analyzer. The electron gun can be rotated in order to change the incident direction of the electron beam with respect to the capillary axis (tilt angle). Since the entrance lens of the analyzer is fixed to have its axis parallel to the capillary axis, the observation angle is fixed at $0^o$ and the acceptance angle depends on the entrance lens focal properties. It should be noted that the azimuthal angle (thus the axis of the capillary with respect to the incident beam) cannot be precisely tuned presently. The schematic view of the experimental setup is shown in Figure 2.

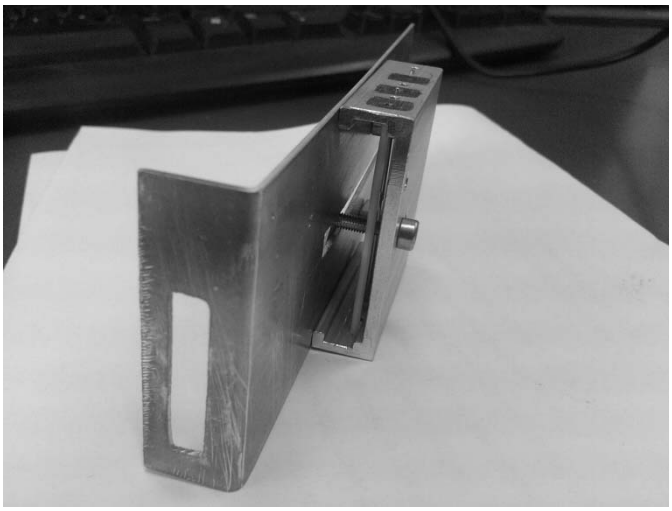

**Figure 1.** A photo of the Teflon capillary sample.

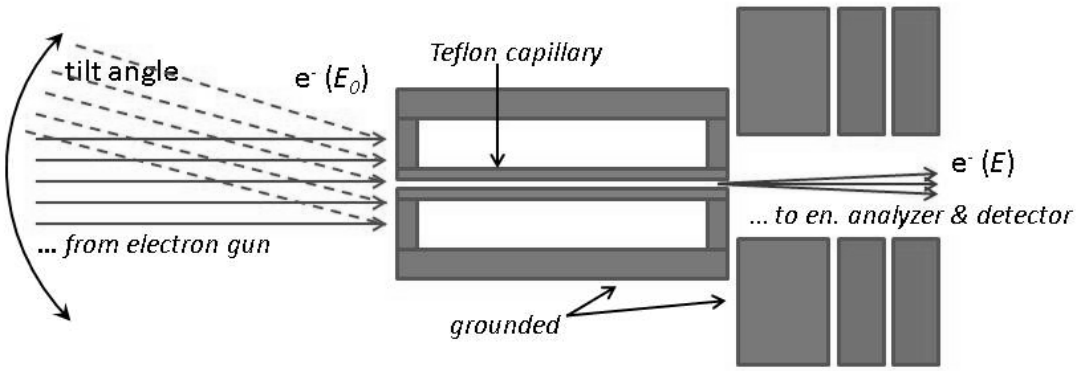


**Figure 2.** Schematic drawing of the experimental setup.

RESULT AND DISCUSSION

The preliminary obtained kinetic energy distribution of low-energy electrons escaping the Teflon capillary at the tilt angle of about $0^o$ and for the incident energy of 200 eV is shown in Figure 3. It should be noted that the results are not corrected for the transmission of the entrance lens of the analyzer. According to our previous experience, this correction reduces the intensity of the electrons close to 0 eV. As shown previously [6,7], the transmission of electrons through an insulating capillary is accompanied with an intensive production of low-energy electrons, due to the close electron-wall interaction. Hereafter, we investigate the angular dependence of the electron current corresponding to the maximum of the low-energy peak from about 0 to 10 eV presented in Figure 3.

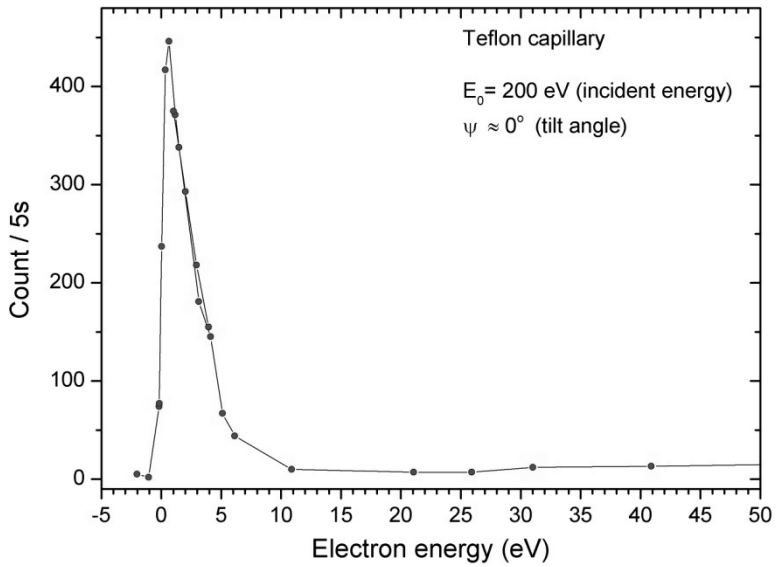


**Figure 3.** Kinetic energy distribution of the low-energy electrons escaping the Teflon capillary.

The angular dependence of the intensity of low-energy electrons escaping the capillary, for the incident energy of 200 eV is presented in Figure 4. In opposite to the case for elastically transmitted electrons (i.e. at the incident energy), where strong tilt angle dependence is always observed, the low-energy electron current is practically independent on the tilt angle in a large range.

The time dependence of the low-energy electron current at the tilt angle of about $0^o$ and for the incident electron energy of 250 eV is shown in Figure 5.

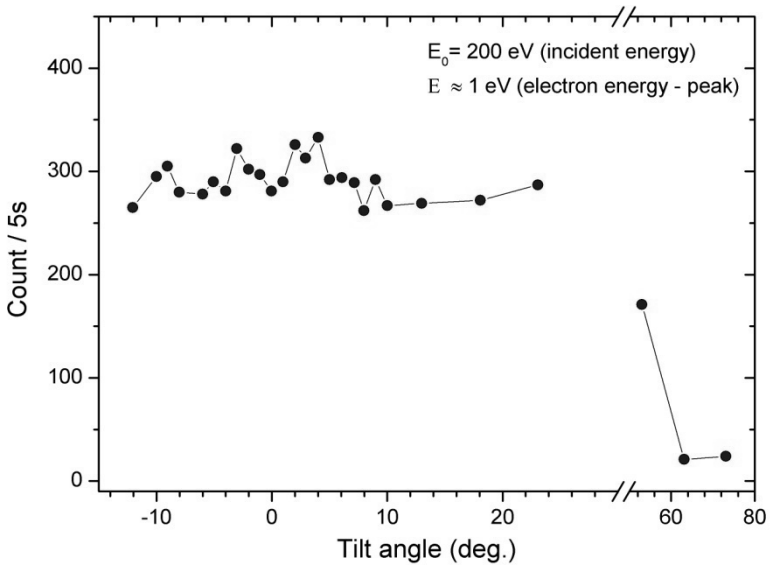


**Figure 4.** Angular distribution of the low-energy electrons escaping the Teflon capillary.

## CONCLUSIONS

We have presented preliminary experimental results on the characterization of low-energy electrons produced upon 200 eV and 250 eV electrons passing the Teflon capillary and escaping through the exit hole. As shown previously, a large intensity of low-energy electrons close to the 0 eV is produced within the capillary due to the close electron-wall interaction. The energy distribution of the electrons is however rather small. Interestingly, the present preliminary measurements suggest a very week dependence of the secondary low-energy electron current escaping the capillary on the tilt angle. This suggests interesting possible applications for the low-energy electron transport. However, further measurements are needed with improved experimental conditions (precise alignment of the capillary axis, characterization of the incident beam, reduced transmission dependence) and different capillary samples.

## ACKNOWLEDGEMENTS

The work was supported by the Ministry of Education, Science and Technical development of Republic of Serbia (Project No. 171020), by the Hungarian Scientific Research Fund OTKA No. NN 103279, and by the Bilateral Cooperation Program between the Hungarian and Serbian Academies.

## REFERENCES

[1] N. Stolterfoht *et al.*, *Phys. Rev. Lett.* **88** 133201 (2002).
[2] C. Lemell *et al.*, *Prog. Surf. Sci.* (2013)
[3] T. Ikeda *et al., J. Phys. Conf. Series* **399** 012007 (2012)
[4] A. Milosavljević *et al.*, *Phys. Rev. A* **75** 030901 (2007).
[5] S. Das *et al.*, *Phys. Rev. A* **76** 042716 (2007).
[6] A. R. Milosavljević *et al.*, *EPL* **86** 23001 (2009).
[7] A. R. Milosavljević *et al.*, *Nucl. Instrum. Meth. B* **279** 190 (2012).

# Calculations of ranges of B, N and H ions during the BN film growth on $Co_{80}Cr_{15}Pt_5$ magnetic layer

B.Tomčik[1], B.P. Marinković[1,2] and B. Predojević[3]
[1]Institute of Physics, University of Belgrade, PO Box68, 11080 Belgrade, Serbia
[2]College for Electrical Engineering and Computing for Vocational Studies, Vojvode Stepe 283, 11000 Belgrade, Serbia
[3]Facullty of Natural Sciences, University of Banja Luka, Republic of Srpska, B&H

**Abstract**
Monte Carlo simulation of the range and distribution of 1000 eV ions of B, N and H into the $Co_{80}Cr_{15}Pt_5$ magnetic layer has been done using the SRIM program. Ranges of B, N and H ions have been determined as 3.3 nm, 2.7 nm and 10.9 nm, respectively. Under the same condition the vacancies produced with boron ions fall in the $10^{-1}$ range, and are similar to nitrogen ($1.13x10^{-1}$) /ion/Angstrom while for hydrogen ions are in $10^{-6}$ ion/Angstrom range. Initial high incident ion energy promotes better film adhesion and keeps sharp interfaces between the new proposed BNx overcoat and the magnetic layer. The insulating property of the overcoat reduces the galvanically induced corrosion current and can extend the life and shelf-time of the hard disks.

**Introduction**
For the hard disk magnetic layer protection against read/write head crash almost exclusively nanolaminated nitrogenated and hydrogenated diamond like carbon films have been used [1]. Mostly, the so called bilayer structure composed of a-C:N film on the top and a-C:H film beneath, close to magnetic layer, is implemented. As the techniques of choice the magnetron sputtering and ion/plasma beam treatments are common[2]. The overall film thickness is bellow 3 nm. As a possible alternative the nano-sized ta-C, BN and SiNx films have been studied. Aside from the magnetic layer mechanical protection, the film corrosion protective resistivity, selective lubricant bondability and a film surface roughness play an important role.

The mixture of hexagonal boron nitride (h-BN) and diamond-like cubic boron nitride (c-BN) is insulating in nature and prevents possible galvanically induced corrosion[3,4]. This chemically and thermally stable overcoat enables self-healing and provides the migrational capabilities of the lubricant layer. Deposition of BN films under equilibrium conditions in most cases studied turned out to be self-limiting to one monolayer. Therefore, ion and plasma beam techniques should be engaged to obtain thicknesses up to 2 nm with the good adhesion to magnetic layer.
During the BN film deposition with borazine$(HBNH)_3$, in liquid state at room temperature, it should be first evaporated and in the gas condition introduced into the vacuum chamber[5]. The low frequency substrate bias should be implemented with the values up to –1000 $V_{DC}$. The estimated influence of the film growth during its initial phase on the magnetic layer has been evaluated by Monte Carlo method. The ion incident energy was 1000 eV and trajectories of 1000 ions have been followed in calculation.

**Results**
**A: Boron**
The stopping range of boron ions is up to 3.3 nm into the magnetic layer, Fig.1a. The black points in the Fig.1b represent the boron ions at the rest, within the magnetic layer matrix.

During the cascade collisions with target atoms boron ions will loose energy on the pathway and some host atoms will be ionized (c), too. It is necessary to investigate whether this will cause the onset of "the magnetic death layer"- lost of magnetic properties of the uppermost magnetic layers.

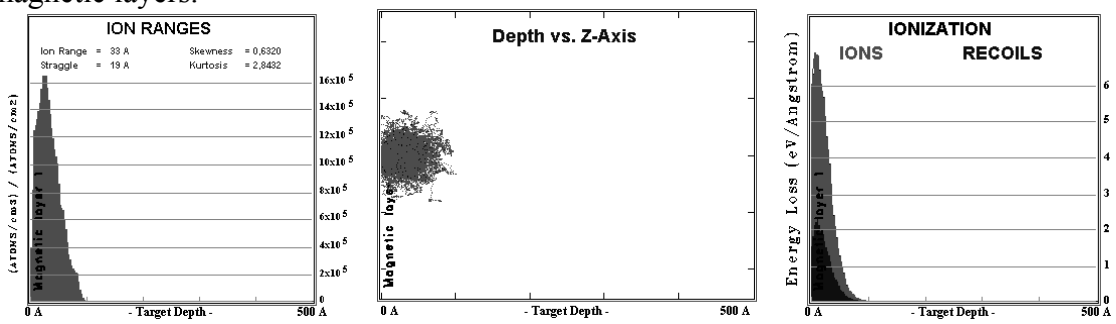


a) b) c)

Fig.1. a) Range, b) distribution under the normal incident angle and c) recoil ionization capabilities of boron ions with energy of 1000 eV into the $Co_{80}Cr_{15}Pt_5$ magnetic layer.

**B: Nitrogen**

The stopping range of 1 KeV nitrogen ions has slightly lower impact during interaction with magnetic layer elements with respect to boron. The ion range distribution is more steep with maximum at $22x10^5$ (atoms/cm$^3$)/(atoms/cm$^2$).

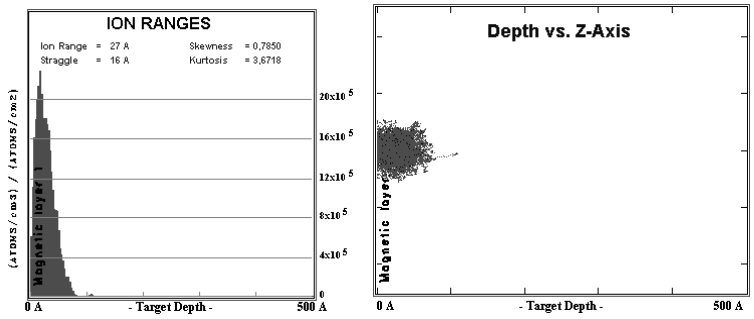


**a) b)**

Fig.2 a) Ion range of nitrogen atoms at 1000 eV incident kinetic energy into the $Co_{80}Cr_{15}Pt_5$ magnetic layer is around 2,7 nm. b) Distribution of nitrogen atoms within the magnetic layer.

**C: Hydrogen**

Small hydrogen ions can penetrate easily into the magnetic layer structure. During film deposition it is to assume that much of hydrogen ions will recombine and leave the film as well as the magnetic layer. Depending on the surface temperature some hydrogen ions will be trapped within the structure. The penetration and scattering depth of hydrogen is usually high.

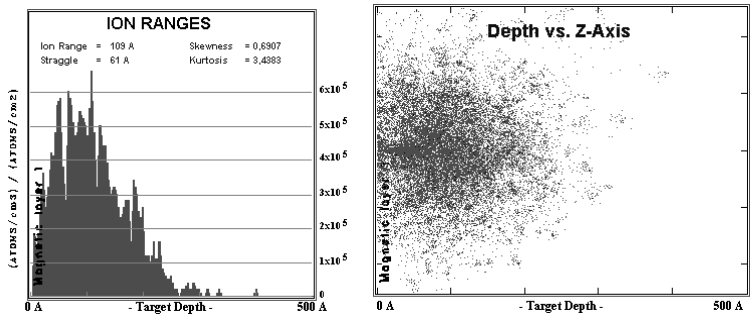


a) b)

Fig.3.Range and propagation/distribution of 1KeV hydrogen ions in the magnetic layer is presented in a) and b), respectively.

The influence of hydrogen ions on the number of vacancies produced within the magnetic layer is very small. Under the same condition the vacancies produced with boron ions fall in the $10^{-1}$ range, and are similar to nitrogen ($1.13x10^{-1}$) /ion/Angstrom. For hydrogen ions vacancies produced are in the $3x10^{-6}$ ions/Angstrom range.

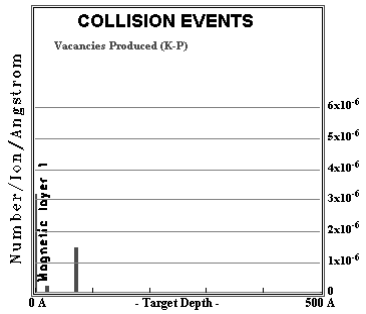


Fig. 4 Vacancies production into the $Co_{80}Cr_{15}Pt_5$ magnetic layer by hydrogen ions, being in the $3x10^{-6}$ /ion/Angstrom range.

## Conclusions

Insulating, high thermal conductivity properties of h-BN and c-BN as well as similarity to carbon overcoat atomic binding gives rise to consider this overcoat as a novel magnetic overcoat layer for the hard disk applications. Unlike high temperature, thermodynamic equilibrium conditions of h-BN film growth that result in a highly ordered monolayer structure it is necessary to use plasma to obtain cross-linked, dense and insulating film at lower substrate temperatures. It is possible to achieve a sharp interface between the BN overcoat and a magnetic layer even at elevated incident energies of B, N and H ions.

## References:

1. Bhushan B, Diamond and Related Materials, Vol. 8(1999)1985-2015

2. J. Robertson, Tribology International, Vol. 36-4-5 (2003)405-415

3. J. J. Pouch, S. A. Alterovitz, Synthesis and Properties of Boron Nitride (Trans Tech Publications, Limited, 1990).

4. Silvan Roth, Fumihiko Matsui,Thomas Greber and Jürg Osterwalder, Nano Lett. 2013, 13, 2668−2675

5. Thomas Greber, e-J. Surf. Sci. Nanotech. Vol. 8 (2010) 62-64